Report

Cell Reports

The Ribosome Cooperates with the Assembly Chaperone pICln to Initiate Formation of snRNPs

Graphical Abstract

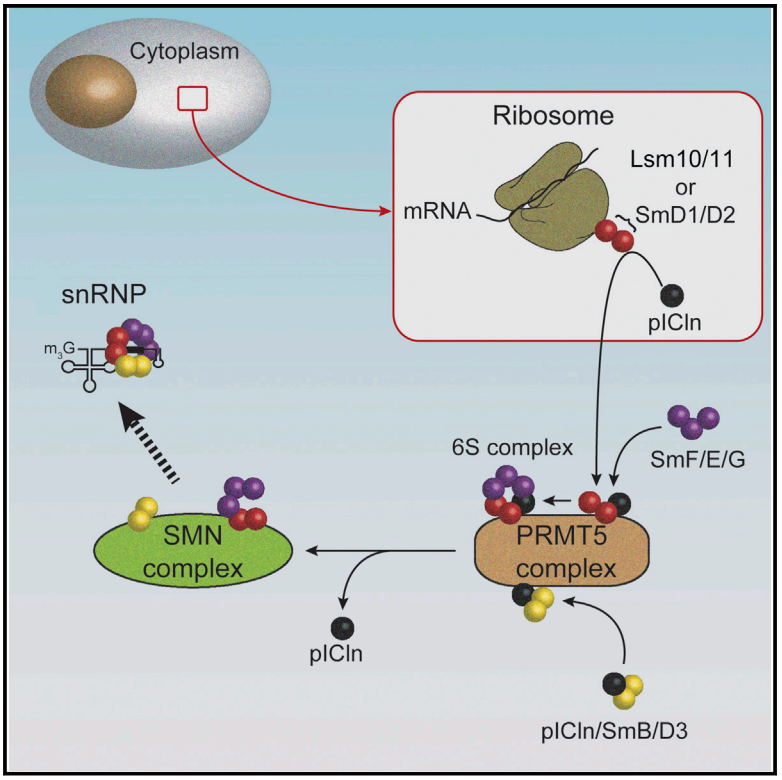

Highlights

- Assembly of macromolecular complexes is initiated at ribosomes
- The assembly chaperone pICln links translation and snRNP assembly
- Ribosomal quality control for the formation of RNA-protein complexes is discovered

Authors

Elham Paknia, Ashwin Chari, Holger Stark, Utz Fischer

Correspondence

ashwin.chari@mpibpc.mpg.de (A.C.), utz.fischer@biozentrum.uni-wuerzburg.de (U.F.)

In Brief

Paknia et al. address how newly synthesized proteins engage with cellular assembly factors to form macromolecular complexes. A role of the ribosome as a quality control hub and a starting point for the assembly process of snRNPs is discovered. The assembly of other macromolecular complexes most likely follows similar principles.

Paknia et al., 2016, Cell Reports *16*, 3103–3112
September 20, 2016
http://dx.doi.org/10.1016/j.celrep.2016.08.047

Cell Reports
Report

The Ribosome Cooperates with the Assembly Chaperone pICln to Initiate Formation of snRNPs

Elham Paknia,[1,2] Ashwin Chari,[2,*] Holger Stark,[2] and Utz Fischer[1,3,4,*]
[1]Department of Biochemistry, University of Wuerzburg, 97074 Wuerzburg, Germany
[2]Department for Structural Dynamics, Max-Planck-Institute for Biophysical Chemistry, 37077 Goettingen, Germany
[3]Department of Radiation Medicine and Applied Sciences, University of California at San Diego, San Diego, CA 92037, USA
[4]Lead Contact
*Correspondence: ashwin.chari@mpibpc.mpg.de (A.C.), utz.fischer@biozentrum.uni-wuerzburg.de (U.F.)
http://dx.doi.org/10.1016/j.celrep.2016.08.047

SUMMARY

The formation of macromolecular complexes within the crowded environment of cells often requires aid from assembly chaperones. PRMT5 and SMN complexes mediate this task for the assembly of the common core of pre-mRNA processing small nuclear ribonucleoprotein particles (snRNPs). Core formation is initiated by the PRMT5-complex subunit pICln, which pre-arranges the core proteins into spatial positions occupied in the assembled snRNP. The SMN complex then accepts these pICln-bound proteins and unites them with small nuclear RNA (snRNA). Here, we have analyzed how newly synthesized snRNP proteins are channeled into the assembly pathway to evade mis-assembly. We show that they initially remain bound to the ribosome near the polypeptide exit tunnel and dissociate upon association with pICln. Coincident with its release activity, pICln ensures the formation of cognate heterooligomers and their chaperoned guidance into the assembly pathway. Our study identifies the ribosomal quality control hub as a site where chaperone-mediated assembly of macromolecular complexes can be initiated.

INTRODUCTION

Recent systematic interaction profiling of the proteome revealed a strong modularity, where most proteins and/or nucleic acids are incorporated into complexes (Gavin et al., 2006). These complexes, on average, contain ten subunits and are composed of proteins alone or proteins and nucleic acids (Gavin et al., 2006). Hence, macromolecular assemblies perform the vast majority of cellular activities. The faithful assembly of these complexes is, therefore, a vital challenge of all cells, and its failure often has profound consequences. The assembly process is often complicated by the fact that many newly synthesized building blocks only attain their folded structure within the context of their respective complex. As a consequence, single subunits have the tendency to misfold, aggregate, or engage in erroneous interactions within the crowded environment of cells. Therefore, the formation of macromolecular complexes in vivo, in many cases, depends on *trans*-acting factors, which sequester individual subunits and safeguard them until incorporated into higher order assemblies (Chari and Fischer, 2010). Indeed, in some cases, the number of *trans*-acting assembly factors exceeds the number of parts to be assembled, as exemplified for the common Sm/Lsm core structure of the pre-mRNA processing small nuclear ribonucleoprotein particles (snRNPs) (Fischer et al., 2011).

Two classes of snRNPs mediate defined pre-mRNA processing reactions in eukaryotes. The first comprises the spliceosomal snRNPs involved in pre-mRNA splicing. They are characterized by a set of seven "Sm" proteins that forms their common structural core. These proteins, termed SmB/B', SmD1, SmD2, SmD3, SmE, SmF, and SmG, encircle a single stranded region of the snRNA (Sm site), to form the Sm core domain. Sm proteins share the Sm-fold, consisting of an N-terminal α-helix followed by a five-stranded antiparallel β sheet. In the assembled Sm core, the β4 strand of one Sm protein connects to a β5 strand of an adjacent Sm protein. This results in the formation of a continuous, intermolecular β sheet among Sm proteins SmE-SmG-SmD3-SmB-SmD1-SmD2-SmF that encloses the Sm site (Kambach et al., 1999). The second class comprises the histone 3′-end processing U7 snRNP, which contains a structurally similar core domain in which the classical Sm proteins SmD1 and SmD2 are replaced by structurally related "like Sm" (Lsm) proteins Lsm10 and Lsm11 (Pillai et al., 2003).

Twelve *trans*-acting factors, united in PRMT5 and SMN complexes, have been linked to snRNPs assembly in vivo. In the early phase, the assembly chaperone pICln binds Sm proteins and delivers them onto the PRMT5 complex (Chari et al., 2008). The assembly pathway then segregates into two lines. In one line, pICln forms a small nuclear RNA (snRNA)-free pseudo-Sm core (termed 6S complex) together with Sm D1, D2, F, E and G, where pICln occupies the position of the remaining two, Sm B/B' and D3. The other line consists of pICln-D3/B, which, unlike 6S, may not dissociate from the PRMT5 complex. In the late phase of snRNP formation, the SMN complex dissociates pICln from Sm proteins and enables their subsequent joining with snRNA (Chari et al., 2008). Formation of the Sm/Lsm core of the U7 snRNP particle appears to follow mechanistically similar

routes (Pillai et al., 2003). In this report, we have addressed the conceptually unresolved question of how newly synthesized Sm/Lsm proteins engage with cellular assembly machineries to evade aggregation and/or mis-assembly. Unexpectedly, we uncovered a role thus far unknown for the ribosome as a quality control hub and a starting point for the chaperone-mediated assembly process. While shown here specifically for snRNPs, these principles may also find use in the assembly of other macromolecular complexes.

RESULTS

Co-sedimentation of Lsm10 and Lsm11 with Polysomes

At steady state, the majority of Sm/Lsm proteins are either associated with the assembly machinery or with snRNP particles (Chari et al., 2008; Meister and Fischer, 2002). To investigate earlier stages of assembly, we generated conditions where the amounts of newly synthesized Sm/Lsm proteins exceeded cellular levels of the essential assembly chaperone pICln. We first focused on the assembly of the U7 snRNP core particle, which consists of the Sm proteins B, D3, E, F, and G, as well as the Lsm10/Lsm11 heterodimer. Tagged Lsm10 and Lsm11 proteins were expressed either alone or in combination by transient transfection, at levels that constitute approximately 20% of the total amount of endogenous Lsm proteins (Figure S1A). Therefore, throughout this article, the conclusions drawn by the analysis of exogenous Lsm proteins are likely to reflect the behavior of the endogenous proteins. Individually expressed proteins localized to the cytoplasm as well as the nucleoplasm (Figure S1B), as described for their endogenous counterparts (Pillai et al., 2001, 2003). As intended, only a small fraction of Lsm10/Lsm11 bound to pICln, as determined by immunoprecipitation (IP) (Figure S1C, lanes 1–8), suggesting that the assembly chaperone pICln was limiting under these conditions. Size fractionation of cellular extracts by gradient centrifugation revealed that pICln sedimented as part of PRMT5 and 6S complexes, as previously reported (Figure 1A, panel a) (Chari et al., 2008). Exogenous Lsm10 sedimented mostly as a free protein (Figure 1A, panel b) and is bound only to substoichiometric amounts of pICln, as shown by IP (Figure S1C, lanes 2, 6, 9, and 10). In contrast, exogenous Lsm11 partially co-sedimented with the PRMT5 complex but was predominantly present in a larger, as-yet-uncharacterized species (Figure 1A, panel c). When both cognate Lsm proteins were co-expressed, the majority of Lsm10 shifted from the top of the gradient to fractions larger than the PRMT5 complex (Figure 1A, panel d). In gradients capable of resolving these heavy fractions, both exogenous Lsm11 (Figure 1B, panel a) and co-expressed Lsm10/Lsm11 (Figure 1B, panel b) were found to co-sediment with ribosomes and polysomes.

Association of Lsm10 and Lsm11 with the Large Ribosomal Subunit

To provide evidence that Lsm10 and Lsm11 in these heavy fractions represent ribosomal/polysomal-associated species, we initially subjected the extract to a prolonged cycloheximide treatment. This treatment led to the general shift of Lsm10/Lsm11 sedimentation from 80S fractions to polysomes (Figure S2A, panels a–c). However, when the extracts were incubated under polysome runoff conditions, a shift of both Lsm proteins to 80S and smaller fractions was elicited (Figure S2A; compare panel b with panel d). Lastly, puromycin treatment of the extract caused Lsm proteins shift from polysomes to 80S fractions (Figure S2B; compare panels a and b). As these treatments selectively modulate the sedimentation behavior of ribosomal species and would not affect the behavior of random aggregates in any manner, these and the following experiments fortify the notion that Lsm11, alone or in complex with Lsm10, associates with the translation machinery.

Next, we analyzed how this ribosomal interaction is established and what significance this may have for snRNP assembly. We found that Lsm11 and the co-expressed Lsm10/Lsm11 dimer stably bound to purified bulk ribosomes, albeit in a substoichiometric manner, as evident by their detection by western blotting but the absence of a recognizable Lsm11 band in Coomassie-stained gels (Figure 1C, lanes 1–4). When ribosomes that contained Lsm10 and Lsm11 were affinity selected from bulk ribosomes with anti-hemagglutinin (HA) antibodies, a stoichiometric complex of Lsm proteins with ribosomes became apparent (Figure 1C, lane 7). The association of Lsm10/Lsm11 with ribosomes/polysomes withstood the treatment with up to 1 M salt and is, therefore, unlikely to be mediated by non-specific electrostatic interactions of the positively charged Lsm proteins with rRNA (Figure 1D; compare lanes 7–13 with lanes 14–20). Moreover, this association was mostly resistant to treatment with 2% detergent (Figure 1D, lanes 21–26). Thus, under conditions of pICln limitation, Lsm proteins associate with ribosomes in a salt- and detergent-resistant manner. Notably, as polysome-bound Lsm11 was detectable by its C-terminal FLAG tag (Figure S2C), this association is not a consequence of translational pausing but reflects the full-length protein bound to ribosomes. Importantly, the amount of full-length endogenous Lsm11 associated with ribosomes/polysomes was increased after the reduction of cellular pICln levels by RNAi (Figure S2D).

To identify the region on the ribosome to which the Lsm proteins bind, cellular extract (Figure 2A, upper panel) and purified ribosomes/polysomes (Figure 2A, lower panel) were treated with micrococcal nuclease (MNase) to digest mRNA. This treatment was found to elicit the shift of Lsm10/Lsm11 from polysomes to 80S ribosomes. The consecutive treatment with MNase and EDTA, which leads to the dissociation of 80S ribosomes, caused the co-sedimentation of Lsm10/Lsm11 with the 60S subunit (Figure 2B, panels a and b). To localize the binding site of the Lsm proteins on the 60S subunit, we performed immuno-electron microscopy (EM) to detect the C-terminal FLAG epitope in Lsm11. Purified MNase-treated 80S ribosomes containing Lsm10/Lsm11 (as in Figure 2A) were incubated with anti-FLAG antibodies at a ratio that led to the predominant formation of two 80S ribosomes bridged by an antibody (Figure 2C, panel a). The region to which anti-FLAG antibodies bound was analyzed on negatively stained electron micrographs (Figure 2C, panels b–d). The antibodies detected full-length Lsm11 on the ribosome in proximity of the polypeptide exit tunnel on the 60S subunit (Figure 2C), i.e., a prominent interaction site for many chaperones, required for folding of nascent proteins and their subsequent release into the cytoplasm.

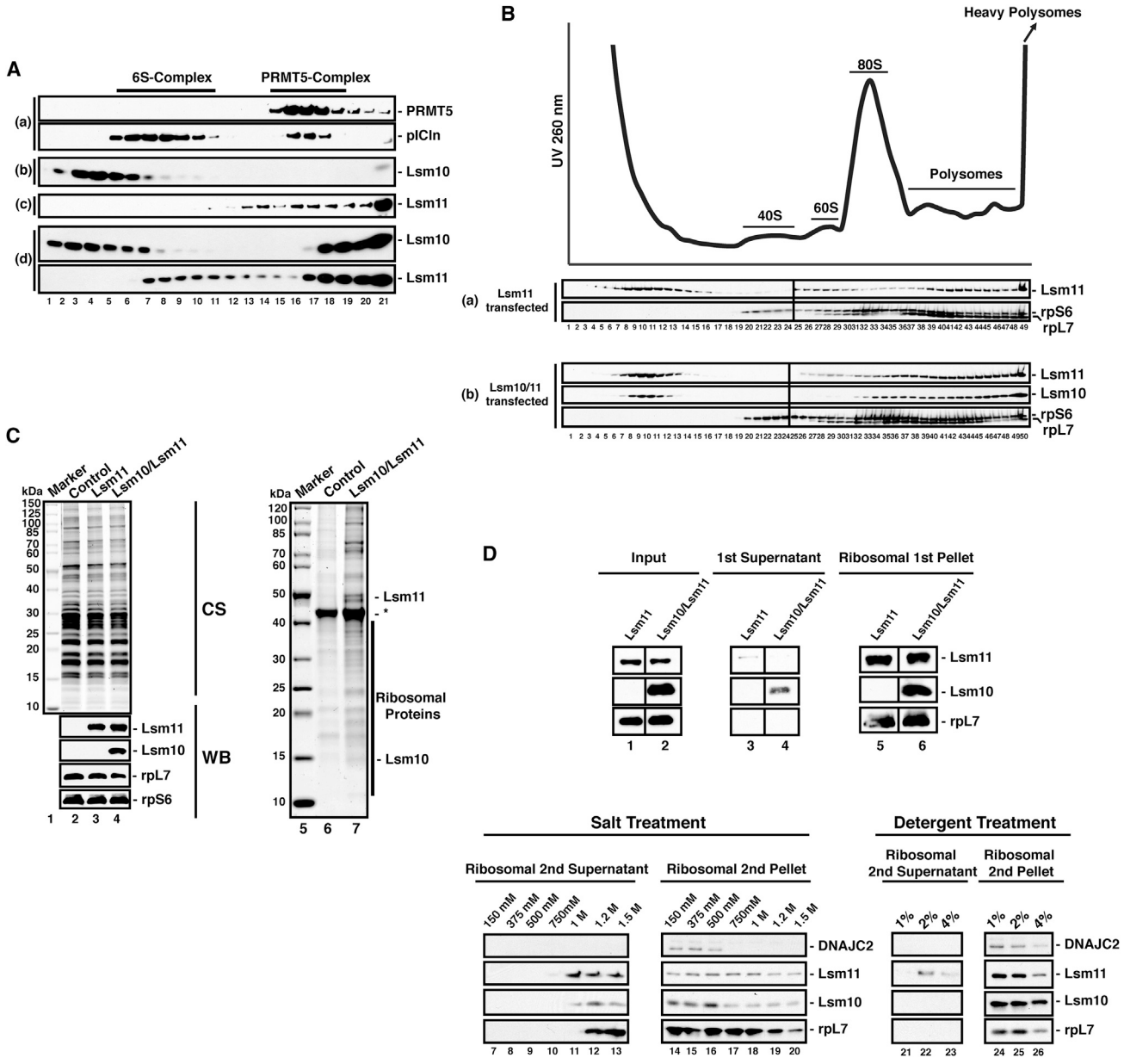

Figure 1. Stable Association of Lsm10 and Lsm11 to Ribosomes

(A) Western blot analysis of cycloheximide-treated extracts fractionated by 10%–30% density gradients with anti-HA, anti-pICln, and anti-PRMT5 antibodies. Cytoplasmic extracts were obtained from cells transfected with plasmids encoding for Lsm10 (b), Lsm11 (c) or both simultaneously (d). (a) depicts a representative western blot of the endogenous PRMT5 and pICln proteins to reveal the sedimentation properties of 6S and PRMT5 complexes, respectively. See also Figure S1C.

(B) 5%–40% high-resolution density gradient centrifugation to resolve high-molecular-weight complexes containing Lsm11 (a) or Lsm10/Lsm11 (b) visible in (A), lanes 19–21. Fractions were analyzed by western blotting with antibodies against HA tag of Lsm10 and Lsm11 and ribosomal proteins L7 and S6 (rpL7 and rpS6, respectively). A UV 260-nm trace revealed the individual ribosomal species (top panel). See also Figure S2C.

(C) Western blot (WB) of purified bulk ribosomes obtained from control, Lsm11-transfected, and Lsm10/Lsm11-transfected cells. The upper panel shows a Coomassie-stained (CS) gel of purified ribosomes from the indicated transfected cells (lanes 1–4), and the lower panel shows immunoblots of the same fractions to detect Lsm10, Lsm11, and ribosomal proteins L7 and S6 (rpL7 and rpS6, respectively) (lanes 1–4). Bulk ribosomes purified from the indicated transfected cells were then subjected to anti-HA immunoprecipitation (IP) to enrich for those with Lsm10/Lsm11 bound. Shown is a Coomassie-stained gel of the respective IPs (lanes 5–7). Note that Lsm10 and Lsm11 appear stoichiometric to ribosomal proteins in the Coomassie-stained gel (lane 7). Asterisk denotes an unidentifed band.

(D) Ribosomes from the indicated transfected cell extracts were purified by differential centrifugation (lanes 1–6), incubated for 30 min with increasing KOAc concentrations at 37°C, and re-sedimented. The pellet and the corresponding supernatants were analyzed by western blotting. Immunoblots against the indicated proteins from ribosomal supernatants (lanes 7–13) and pellets (lanes 14–20) are shown. The same experiment was performed with the addition of 1%, 2%, and 4% NP-40 instead of salt. Immunoblots against the indicated proteins from ribosomal supernatant (lanes 21–23) and pellets (lanes 24–26) are shown.

pICln Only Releases the Cognate Lsm10/Lsm11 Heterodimer from Ribosomes

The association of mature Lsm proteins with the ribosome may represent the starting point in the snRNP assembly. If so, one would predict that (1) the cognate Lsm10/Lsm11 heterodimer is formed at the ribosomal exit tunnel and that (2) the assembly chaperone pICln enables its ordered transfer onto the PRMT5 complex. As shown earlier, Lsm11 was able to establish the interaction to ribosomes on its own, whereas Lsm10 required the co-expression of Lsm11 for binding (Figure 1A [compare panel b with panel d]; Figure 1B). To verify that the ribosomal association of Lsm10 was dependent on Lsm11, a mutant of Lsm11 (Lsm11ΔSm2) lacking the binding region for Lsm10 was tested. While this mutant was still able to associate with ribosomes/polysomes, it failed to recruit Lsm10 upon co-transfection (Figure S2E). Next, we investigated whether pICln was able to release a cognate Lsm10/Lsm11 heterodimer from its ribosomal site of formation. For this, we co-expressed pICln either with Lsm11 alone (Figure 3A, panel a), the cognate Lsm10/Lsm11 dimer (Figure 3A, panel c), or the non-cognate proteins Lsm11 and SmD1 (Figure 3A, panel d), and respective extracts were size fractionated. Co-transfection of pICln caused efficient ribosomal release of the Lsm10/Lsm11 heterodimer, as evident by its redistribution from polysomes to lighter fractions of the gradient (Figure 3A; compare panels b and c). pICln failed, however, to dissociate Lsm11 alone (Figure 3A, panel a) or co-expressed Lsm11 and SmD1 (Figure 3A, panel d). Furthermore, when Lsm11ΔSm2, which is incapable of forming the Lsm10/Lsm11 heterodimer, was co-expressed with Lsm10, pICln could not promote its release from the ribosomes (Figure S3A).

In high-resolution density gradients, the Lsm10/Lsm11 heterodimer, which was released by the co-transfection of pICln, was found to co-sediment with pICln in the 6S–20S region of the gradient (i.e., the size range of 6S and PRMT5 complexes; Figure S3B, lanes 2–12). Additionally, purified bulk ribosomes contained markedly reduced levels of Lsm10/Lsm11 proteins upon pICln co-transfection (Figure S3C; compare lanes 3 and 4), which was confirmed by IP (Figure S3C; compare lanes 5 and 6). These experiments illustrate the strict requirement for cognate Lsm heterodimer formation for pICln-driven ribosome release.

Newly Translated Lsm10 and Lsm11 Proteins Interact with pICln at the Ribosomes

Next, we asked whether pICln released newly synthesized Lsm proteins from ribosomes rather than from a pre-existing cellular pool thereof. We pulse-labeled either non-transfected cells or cells co-expressing Lsm10/Lsm11, using [^{35}S]-methionine. Bulk ribosomes were then purified from these cells, and pICln was added. Ribosomes were then pelleted, and Lsm10/Lsm11 was immunoprecipitated from the supernatant and analyzed by western blotting (Figure 3B, lanes 1 and 2) and autoradiography (Figure 3B, lanes 3 and 4). This revealed that pICln released labeled and, therefore, newly synthesized Lsm10/Lsm11 heterodimer from ribosomes. The formation and accumulation of Lsm10/Lsm11 on ribosomes, hence, represents the earliest as-yet documented intermediate in snRNP assembly.

Next, it was of interest to test whether pICln alone was sufficient for ribosomal release of the cognate Lsm10/Lsm11 heterodimer. We purified ribosomes from cells co-transfected with Lsm10 and Lsm11 and added increasing amounts of recombinant pICln (Figure 3C, upper panels). We found that pICln (lanes 4–6, 8, and 14–15), but neither non-related control proteins nor small molecules (lanes 7, 9–12, and 16) released ribosome-associated Lsm10/Lsm11 in a dose-dependent manner and without the requirement of metabolic energy. Surprisingly, the pICln-dependent release of the Lsm10/Lsm11 heterodimer occurred quantitatively under physiological salt conditions, despite the salt-resistant interaction of the Lsm10/Lsm11 heterodimer with ribosomes.

pICln Links the Translation of Lsm10/Lsm11 with RNP Assembly

The dissociation of ribosome-bound Lsm10/Lsm11 by pICln results in the formation of a pICln/Lsm10/Lsm11 complex. This unit is analogous to the short-lived building block pICln/SmD1/SmD2, which binds the PRMT5 complex and matures into the 6S complex of spliceosomal snRNPs (Chari et al., 2008; Neuenkirchen et al., 2015). Hence, we asked whether pICln/Lsm10/Lsm11 released from the ribosome could be converted into intermediates that resemble PRMT5 and 6S complexes. Upon co-transfection, pICln, Lsm10 and Lsm11 were, indeed, found to co-sediment in fractions corresponding to these complexes (Figure 3D). Anti-FLAG IPs from these fractions enabled us to characterize the U7 snRNP assembly intermediates (Figure 3E, lanes 1–4). Immunoblotting (Figure 3E, lanes 5 and 6) and mass spectrometry (Table S1) revealed that the 20S peak contained the PRMT5 complex bound to Lsm10/Lsm11 and all spliceosomal Sm proteins. In contrast, the U7-specific 6S complex consists of pICln, SmE/SmF/SmG, and Lsm10/Lsm11 (Pillai et al., 2001, 2003). Thus, pICln-mediated ribosomal release of the Lsm10/Lsm11 heterodimer primes these proteins for U7 snRNP assembly by the formation of distinct intermediates.

Finally, we wanted to investigate whether the formation of spliceosomal snRNPs likewise entails an early ribosome-associated phase as described earlier for the U7 particle. Hence, we investigated the fate of the Lsm10/Lsm11 paralogs, SmD1/SmD2, upon reduction of pICln levels by RNAi (Figure 4A, left panel). A strong association of SmD1/SmD2 with ribosomes and polysomes became apparent upon pICln reduction in comparison to the mock-transfected control (Figure 4A, panels a and b). Conversely, the restoration of pICln levels by transfection of exogenous HA-pICln selectively reduces ribosomal SmD1/SmD2 both in control and pICln-siRNA (small interfering RNA)-transfected cells (Figure 4A, panels c and d). Additionally, exogenous pICln was able to release the SmD1/SmD2 heterodimer from the purified ribosomes (Figure S3D). Thus, not only Lsm10/Lsm11 but also SmD1/SmD2 proteins remain bound to the ribosome as full-length proteins and are only released in a pICln-mediated reaction when the respective cognate Sm/Lsm heterooligomers have formed.

DISCUSSION

In this study, we have elucidated how newly synthesized Sm/Lsm proteins are incorporated into the assisted assembly

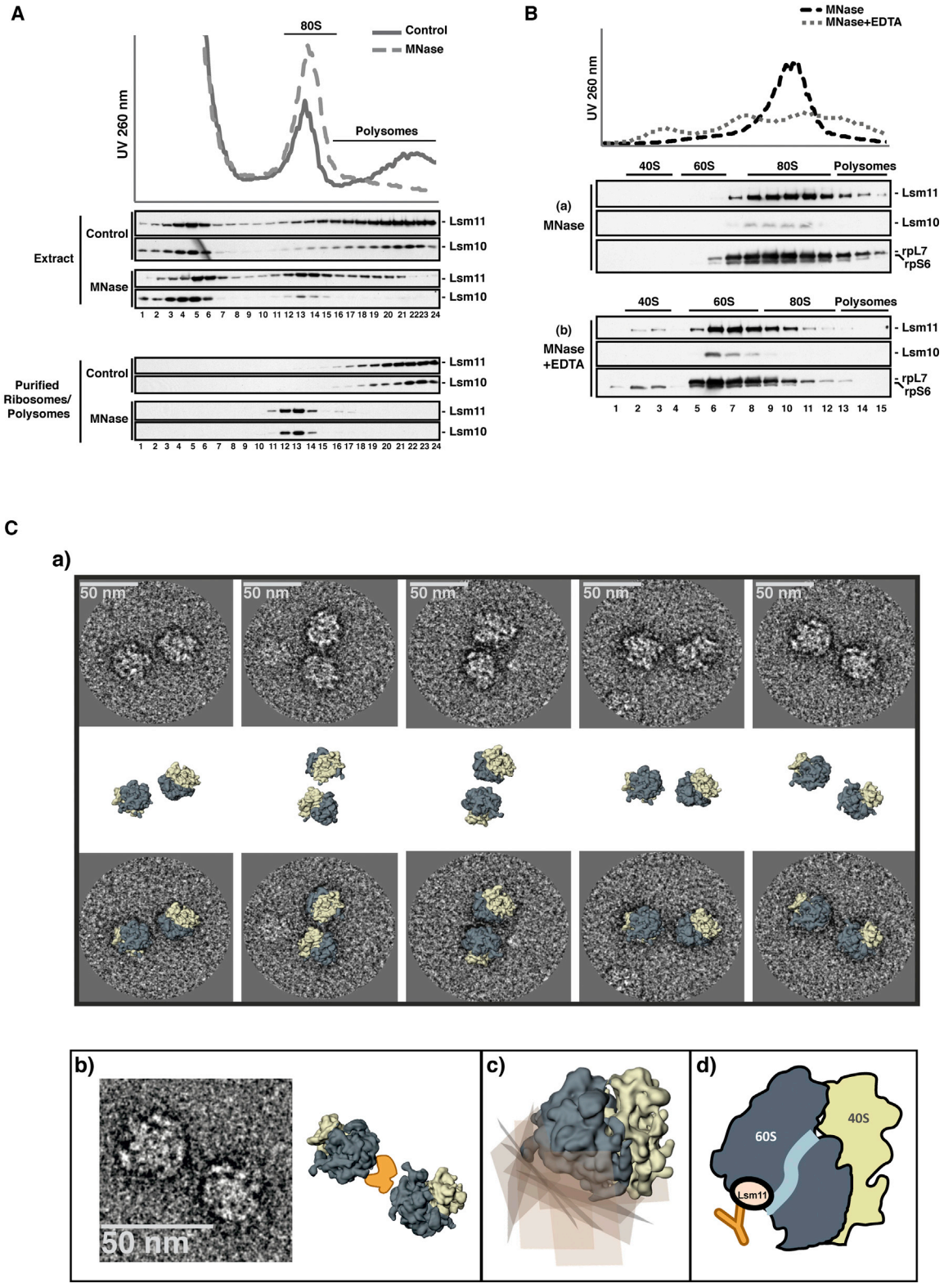

Figure 2. Retention of Full-Length Lsm Proteins in Proximity of the Ribosomal Exit Tunnel

(A) Western blot analysis of cytoplasmic extracts fractionated by density gradient upon mock (control) or micrococcal nuclease (MNase) treatment (upper panel). The same experiment as in the upper panel, however, using purified ribosomes/polysomes is shown in the lower panel. Note the absence of Lsm10/Lsm11

(legend continued on next page)

pathway of snRNPs. Our data suggest that full-length SmD2 and Lsm11 proteins initially remain bound to the ribosome at a site in proximity to the polypeptide exit tunnel (Figure 4). While the sequestration of nascent polypeptides on the ribosome elicited by stalling has been described previously (Albanèse et al., 2006; Gong and Yanofsky, 2002; Keenan et al., 2001; Mariappan et al., 2010; Schuldiner et al., 2008), to our best knowledge, the interaction of Sm/Lsm proteins documented here represents the first observation of full-length proteins being retained in proximity to the polypeptide exit tunnel. The interaction with the ribosome is mediated by Lsm11 and, by analogy, SmD2. However, both proteins cannot directly interact with the assembly chaperone pICln (Chari et al., 2008; Grimm et al., 2013). Thus, to proceed in the pathway, two prerequisites must be met: (1) formation of a cognate Lsm10/Lsm11 or SmD1/SmD2 heterodimer (Figure 4B, Ia and IIa) and (2) the interaction with pICln mediated by Lsm10 and SmD1, respectively (Figure 4B, Ib and IIb). This prevents an un-chaperoned release into the cytosol and leads to the ordered formation of pICln/SmD1/SmD2 and pICln/Lsm10/Lsm11 (Figure 4B, Ic and IIc). Of note, both complexes pre-determine the subsequent assembly pathway: whereas the pICln/Lsm10/Lsm11 complex is converted at the PRMT5 complex into a 6S complex predestined for U7 snRNPs (i.e., pICln/Lsm10/Lsm11/SmF/SmE/SmG; Figure 4B, Id), pICln/SmD1/SmD2 forms the 6S complex specific for spliceosomal snRNPs (i.e., pICln/SmD1/SmD2/SmF/SmE/SmG; Figure 4B, IId). Thus, the orchestration of consecutive specific protein-protein interactions on the ribosome drives early events in the assembly pathway.

Recent studies depict the ribosome as a central hub, where productive protein folding is integrated with both protein and mRNA quality control (Harigaya and Parker, 2010; Pechmann et al., 2013; Rodrigo-Brenni and Hegde, 2012). Subunits of macromolecular assemblies often display hydrophobic interaction surfaces with a high tendency for aggregation with non-cognate cellular components (Chari and Fischer, 2010; Ellis, 2013). Therefore, it appears appropriate that specialized assembly pathways for newly synthesized subunits should be initiated at the ribosome itself. Although the results presented here are highly specific for snRNPs, the same principles are likely to apply to the assembly of other macromolecular complexes as well. Our findings indicate that the coordinated hand-off of newly translated proteins from the ribosome to dedicated assembly chaperones might be a widespread phenomenon in ensuring faithful macromolecular complex assembly in living cells. The recent finding of co-translational assembly of operon-encoded luciferase subunits LuxA and LuxB in *E. coli* suggests that similar mechanisms described here for eukaryotes may likewise account for macromolecular complex formation in prokaryotes (Shieh et al., 2015).

EXPERIMENTAL PROCEDURES

Cell Culture and Cytoplasmic Extract Preparation

293T cells were grown, maintained at 37°C, and transfected with Nanofectin at 70%–80% confluency (PAA Laboratories). Transfection of siRNA was performed with Lipofectamine RNAiMAX (Invitrogen).

To prepare cytoplasmic extracts, cells were washed and re-suspended in lysis buffer (50 mM HEPES-KOH (pH 7.5), 120 mM KOAc, 5 mM $Mg(OAc)_2$, 5 mM DTT, 100 U/ml RNasin, and protease inhibitors) containing 0.5% (v/v) NP-40. In cases where polysomes were analyzed, cells were incubated with 100 μg/ml cycloheximide at 37°C for 15 min, and the lysis buffer additionally contained 100 μg/ml cycloheximide. The cells were incubated for 20 min on ice and inverted every 5 min. Lysates were cleared by centrifugation at 13,000 rpm for 15 min at 4°C in a table-top centrifuge. Extracts were always prepared fresh prior to each experiment.

Purification of Ribosomes

For ribosome purification, 293T cytoplasmic extract was filtered through a 0.45-μm syringe filter (Pall) and then layered on a 45% (w/v) sucrose cushion in cushion/gradient buffer (50 mM HEPES-KOH (pH 7.5), 120 mM KOAc, 5 mM $Mg(OAc)_2$, 5 mM DTT, and 10 μg/ml cycloheximide). The cushion was subjected to centrifugation at 70,000 rpm at 4°C for 2 hr in a TLA 100.3 rotor (Beckman Coulter). Afterward, the supernatant was decanted and transferred to a fresh tube. The pellet was washed with PBS or re-suspension buffer (50 mM HEPES-KOH [pH 7.5], 120 mM KOAc, 5 mM $Mg(OAc)_2$, and 5 mM DTT). The pellet was gently re-suspended in PBS in the case where the re-suspended pellet was directly subjected to SDS-PAGE or in re-suspension buffer in the case where the re-suspended pellet was used for further functional experiments. Re-suspension was achieved by adding buffer to the pellet and gentle shaking on a rotary shaker for 2 hr at 4°C so that no frothing occurred.

Density Gradient Centrifugation

All gradients were prepared with a Biocomp Gradient Master (Science Services). To resolve 6S and PRMT5 complexes, 293T extract was layered on top of linear 10%–30% (w/v) galactose gradient in PBS buffer. Gradients were subjected to centrifugation at 40,000 rpm for 16 hr at 4°C in SW 60Ti rotor (Beckman Coulter) and harvested manually. To obtain 40S, 60S, 80S, and polysomal fractions, 293T extract was layered on top of a 5%–45% (w/v) sucrose gradient in gradient/cushion buffer. Gradients were subjected to centrifugation at 34,500 rpm for 2 hr at 4°C in a SW 41Ti rotor (Beckman Coulter). Gradients were harvested on a Biocomp Piston Gradient Fractionator (Science Services).

To resolve 40S, 60S, and 80S ribosomes, extracts were layered on 5%–45% (w/v) sucrose gradients in gradient/cushion buffer and sedimented at 17,000 rpm for 16 hr at 4°C in a SW 60Ti rotor (Beckman Coulter) and harvested manually. For high-resolution gradients, 293T extract was

apparently sedimenting in sub-ribosomal fractions when purified ribosomes/polysomes are utilized (compare upper and lower panels). UV traces on top of the gradients revealed the migration of ribosomal species in each gradient.

(B) Western blot analysis of cytoplasmic extracts fractionated by density gradient centrifugation. Extracts obtained from cells co-transfected with Lsm10/Lsm11 were treated with either MNase (a) or MNase and EDTA (b) to study the sedimentation pattern of Lsm10/Lsm11. Note that only the fractions corresponding to ribosomal subunits and polysomes are shown. UV traces on top of the gradients revealed the migration of ribosomal species in the each gradient. See also Figures S2A and S2B.

(C) 80S-antibody-80S trimeric complexes were purified from 293T cytoplasmic extracts according to Experimental Procedures. The concentration of complexes on the EM grid was intentionally kept low to make sure that the 80S ribosomes were juxtapositioned by the anti-FLAG antibodies and not coincidentally positioned next to each other (upper lane of a). The orientation of 80S ribosomes within the 80S-antibody-80S complex was evaluated based on the known structure of human 80S ribosomes (lower lane of a). Single raw image and schematic of ribosomes juxtaposed by the anti-FLAG antibody (b). The exact binding site of the antibody at the interface between two 80S ribosomes cannot be exactly determined in a single image. Rectangles were thus modeled to the 80S structure at the respective binding site of the antibody in position for ribosome-bound HA-Lsm11-FLAG, which is in proximity to the polypeptide exit tunnel (c). A schematic representation of the Lsm11 binding site on the ribosome is shown (d).

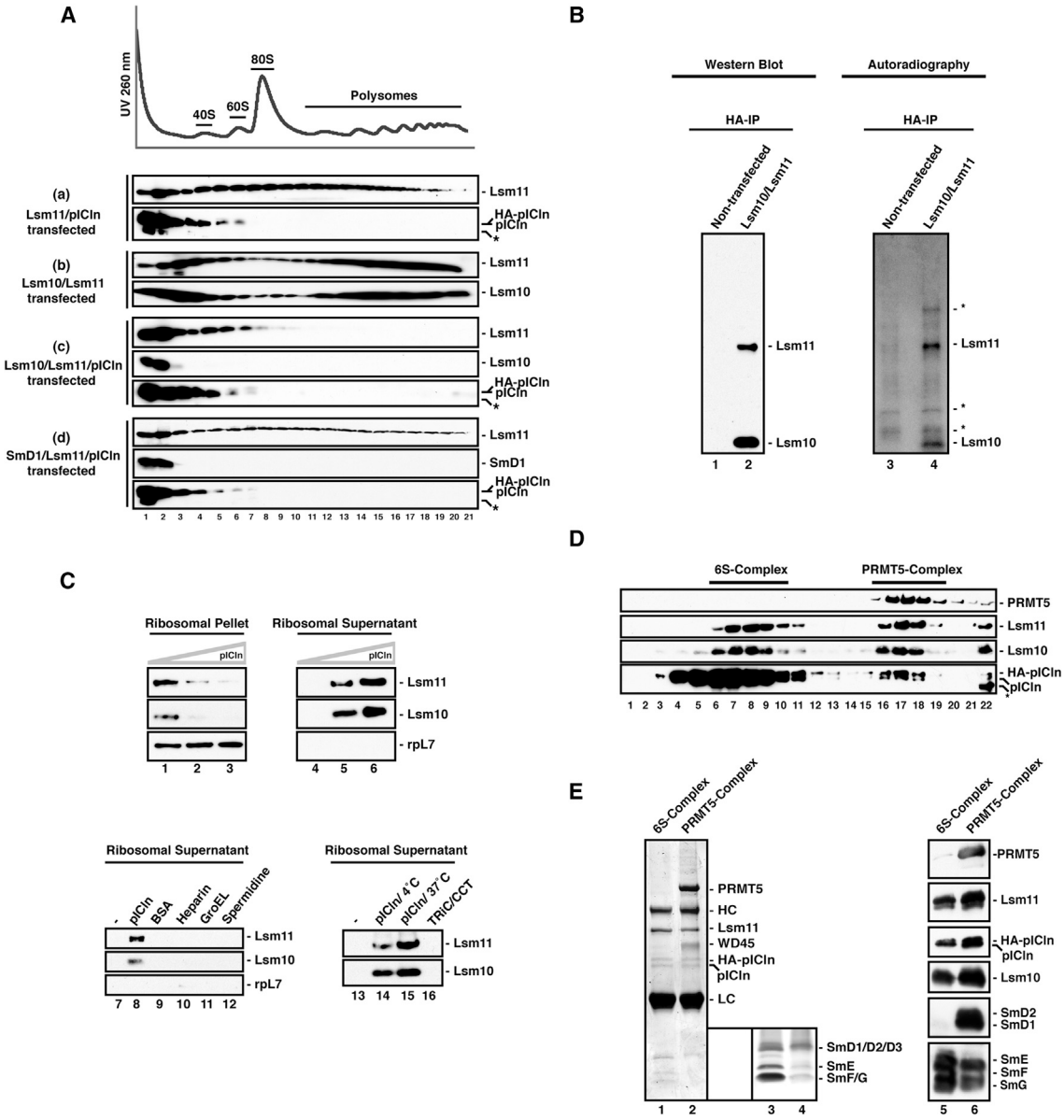

Figure 3. U7 snRNP Assembly Is Initiated Already at the Ribosome

(A) Cells were co-transfected with plasmids encoding either for Lsm11 and pICln (a), Lsm10/Lsm11 (b), Lsm10/Lsm11 and pICln (c), or SmD1/Lsm11 and pICln (d). Extracts derived from these cells were separated by gradient centrifugation and analyzed by western blotting with anti-HA antibody to detect Lsm and Sm proteins. To detect pICln, anti-pICln antibodies were used. A representative ribosomal profile is shown in the top panel. Asterisk denotes an unidentified band. See also Figures S3B and S3C.

(B) Either non-transfected cells or cells co-transfected with Lsm10 and Lsm11 were pulse-labeled with [^{35}S]-methionine, bulk ribosomes were purified by differential centrifugation, and purified recombinant pICln was added. After incubation, ribosomes were re-sedimented, and the supernatants were additionally immunoprecipitated with anti-HA beads and resolved by SDS-PAGE. Shown are immunoblots and the corresponding autoradiography of the anti-HA immunoprecipitates from non-transfected cells (lanes 1 and 3, respectively) or cells simultaneously co-transfected with Lsm10 and Lsm11 (lanes 2 and 4, respectively). Asterisk denotes an unidentified band.

(C) Lsm10/Lsm11-containing ribosomes were incubated with increasing concentrations of pICln and subjected to differential centrifugation. Western blots of the individual ribosomal pellets (lanes 1–3) and corresponding supernatants (lanes 4–6) using antibodies against HA tag or ribosomal protein L7 (rpL7) are shown. The same ribosomal release reaction as in lanes 1–6 was performed with mock, pICln, BSA, heparin, GroEL, spermidine (lanes 7–13), and TRiC/CCT (lane 16) treatment. See also Figure S3E.

(legend continued on next page)

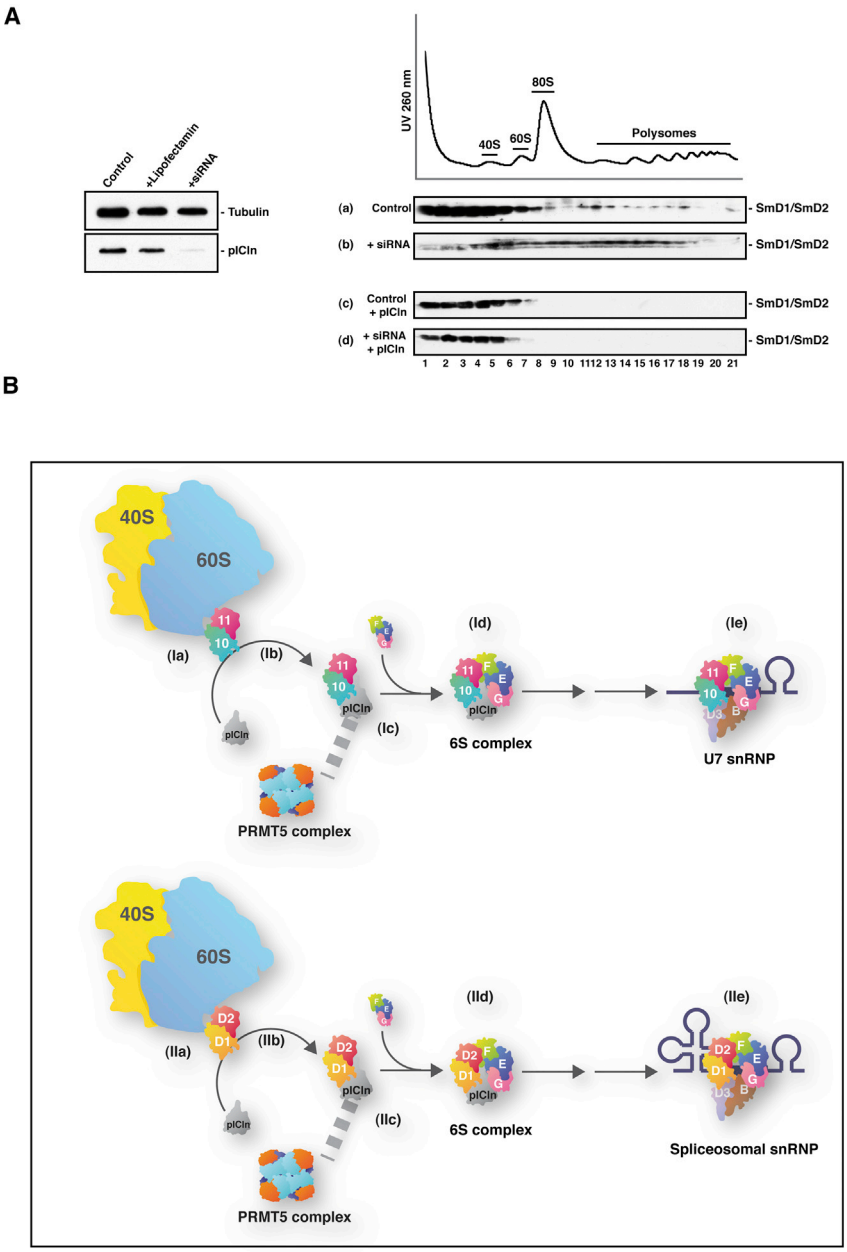

Figure 4. pICln Releases the Canonical SmD1/D2 Heterodimer from the Ribosome

(A) Extracts prepared from non-transfected control cells and cells transfected with a siRNA pool directed against pICln mRNA were used. Left panel shows western blot analysis using antibodies against pICln and tubulin as a loading control. Right panels show the sedimentation analysis of endogenous SmD1/SmD2 in extracts of control cells (a), pICln-depleted cells (b), pICln-overexpressing control cells (c), and cells in which the depleted endogenous pICln pool was replenished upon exogenous pICln expression (d). See also Figure S3D.

(B) A schematic model of the earliest cellular snRNP assembly stages. Newly translated Lsm11 and SmD2 proteins are not released from the ribosome but require the formation of a cognate Sm/Lsm protein heterodimer (steps Ia and IIa, respectively). The assembly chaperone pICln then binds and dissociates the cognate heterodimer (steps Ib and IIb), leading to the formation of pICln/Lsm10/Lsm11 (step Ic) or pICln/SmD1/SmD2 (step IIc). Both units are then bound to the PRMT5 complex, where they are converted to either the U7-specific (step Id) or spliceosomal (step IId) 6S complexes upon the addition of SmE/SmF/SmG. The U7 snRNP (step Ie) or spliceosomal snRNPs (step IIe) are formed by the dissociation of pICln and the addition of the respective snRNA at the SMN complex (data not shown; see also Discussion).

layered on top of a 5%–40% (w/v) sucrose gradient in gradient/cushion buffer and sedimented at 40,000 rpm for 4 hr at 4°C in a SW 40Ti rotor (Beckman Coulter).

MNase, Puromycin Treatment of Extracts, and Translation Runoff Experiment

Cytoplasmic extracts and/or purified ribosomes/polysomes were supplemented with $CaCl_2$ to a final concentration of 2 mM. 150 U MNase was added, and extracts and/or purified ribosomes/polysomes were incubated at 20°C for 30 min. For the combined treatment of extracts with both MNase and EDTA, the latter was added to a final concentration of 50 mM. Treated samples were then layered on 5%–45% (w/v) sucrose gradients and centrifuged at 17,000 rpm for 16 hr at 4°C in a SW 60Ti rotor, as in Figure 2B, or at 34,500 rpm for 2 hr at 4°C in a SW 40Ti rotor, in Figure 2A. Individual fractions were analyzed by SDS-PAGE and western blotting.

To study the effect of puromycin, cells were incubated with 5 mM puromycin for 30 min prior to preparation of the extract, and lysis buffer contained 5 mM puromycin. Extract was layered on a 40% sucrose cushion containing 1 mM puromycin, and ribosomes were pelleted as described earlier. Ribosomal pellets were re-suspended in re-suspension buffer containing 1 mM puromycin. Re-suspended ribosomes were further incubated at room temperature in the presence of 5 mM puromycin and 250 mM salt for 30 min before fractionation on a 5%–45% sucrose gradient.

To run off translation, cells co-transfected with Lsm10 and Lsm11 were incubated with 100 μg/ml cycloheximide for 2 hr at 37°C. Extract was prepared and incubated at 37°C for 2 hr in the presence of 5 mM ATP and 100 U/ml RNasin.

(D) Plasmids encoding Lsm10, Lsm11, and pICln were co-transfected into cells and subsequently analyzed by gradient centrifugation and western blotting, as described in Figure 1A. The fractions corresponding to 6S and PRMT5 complexes are indicated.

(E) Coomassie-stained gel (lanes 1 and 2) and western blot analysis (lanes 5 and 6) of co-purified proteins associated with HA-Lsm11-FLAG in 6S- and PRMT5-complex fractions shown in (D). The inset (lanes 3 and 4) shows a silver-stained portion of the same gel for better appreciation of low-molecular-weight proteins. See also Table S1.

Ribosome Release Reactions with pICln

Cytoplasmic extracts were prepared from 293T cells transfected with the indicated plasmids. Extracts were subjected to differential centrifugation, and ribosomal pellets were carefully re-suspended as described earlier. The UV absorption at 260 nm was measured, and the concentration of ribosomes was determined by using the conversion factor, which assumes that one OD_{260} (optical density at 260 nm) unit corresponds to 20 pmol of ribosomes. For ribosome release reactions, increasing amounts of recombinant pICln (Chari et al., 2008) (0-, 5-, and 50-fold molar excess over ribosomes), control proteins, or small molecules (at 50-fold molar excess over ribosomes) were added to a constant amount (150–200 pmol) of re-suspended ribosomes. The reaction was incubated for 30 min at 37°C. Immediately after the completion of incubation, the reaction tubes were transferred to ice, and an equal volume of re-suspension buffer was added. The reaction was then subjected to differential centrifugation as described earlier, and supernatants and re-suspended pellets were analyzed by western blotting.

Pulse Labeling

Cells co-transfected with plasmids encoding Lsm10 and Lsm11 or non-transfected cells were used. 24 hr after transfection, the medium was removed, and cells were washed with medium without methionine. Afterward, cells were incubated with medium without methionine for 1 hr (starvation). Thereafter, the medium was removed, and cells were incubated with medium containing [^{35}S]-methionine at a concentration of 20 μCi/ml for 1 hr. Extracts were prepared as described earlier.

Immuno-EM

For immuno- EM sample preparation, cytoplasmic extracts prepared from 293T cells co-transfected with HA-Lsm10 and HA-Lsm11-FLAG were subjected to MNase treatment as described earlier. Subsequently, ribosomes were isolated by differential centrifugation as described earlier. For labeling with antibodies, ribosomes containing HA-Lsm10 and HA-Lsm11-FLAG were re-suspended and incubated with different concentrations of anti-FLAG antibody. The antibody concentration, which yielded the highest proportion of 80S-antibody-80S trimers was then empirically determined by negative-stain EM. These trimers were then enriched by 5%–45% (w/v) sucrose gradients run at 17,000 rpm for 16 hr in a SW 60Ti rotor (Beckman Coulter) at 4°C. The appropriate fraction was then re-analyzed by negative-stain EM, as described previously (Chari et al., 2008). Images were recorded on a Philips CM200 electron microscope (Philips/FEI) operated at 160 kV using a 2-fold-binned 4kx4k CCD (charge-coupled device) camera (TemCam-F415, TVIPS) at a magnification of 119,000-fold, resulting in a pixel size of 2.5 Å. The concentration of particles on the EM grid was chosen to be very low to ensure that 80S dimers were not formed accidentally by high concentrations of ribosomes. Fifty 80S-antibody-80S trimers were selected to determine the Lsm11 binding site on the ribosome. The projection direction of each 80S ribosome was determined, and a rectangular plane was drawn in 3D, perpendicular to the imaging plane at the antibody-binding site (Figure 2C). The x and y dimensions of the rectangular planes reflect the uncertainties of detecting the binding site of the antibody. The overlapping area of all rectangular planes, therefore, describes the position of the anti-FLAG antibody. We were thus able to determine the location of the Lsm11 binding site on the ribosome and find it to lie in proximity to the polypeptide exit tunnel as shown in Figure 2C.

SUPPLEMENTAL INFORMATION

Supplemental Information includes Supplemental Experimental Procedures, three figures, and one table and can be found with this article online at http://dx.doi.org/10.1016/j.celrep.2016.08.047.

AUTHOR CONTRIBUTIONS

E.P., A.C., and U.F. conceived and designed the project. E.P. performed all biochemical experiments with the help of A.C. E.P., A.C., and H.S. prepared samples for EM. A.C. and H.S. analyzed the EM data. E.P., A.C., and U.F. wrote the manuscript with the help of H.S. All authors discussed the results and commented on the manuscript.

ACKNOWLEDGMENTS

We thank A. Buchberger, B. Kastner, M. Rodnina, and R. Lührmann for helpful comments on the manuscript and providing reagents. We are grateful to W. Liu and R. Meduri for drawing the models and M. Raabe and H. Urlaub for performing mass spectrometry analysis. This work was supported by DFG grants Fi573/8-1 and CH1098/1-1. E.P. was supported by a grant from the GSLS Wuerzburg.

Received: May 11, 2016
Revised: July 11, 2016
Accepted: August 15, 2016
Published: September 20, 2016

REFERENCES

Albanèse, V., Yam, A.Y., Baughman, J., Parnot, C., and Frydman, J. (2006). Systems analyses reveal two chaperone networks with distinct functions in eukaryotic cells. Cell *124*, 75–88.

Chari, A., and Fischer, U. (2010). Cellular strategies for the assembly of molecular machines. Trends Biochem. Sci. *35*, 676–683.

Chari, A., Golas, M.M., Klingenhäger, M., Neuenkirchen, N., Sander, B., Englbrecht, C., Sickmann, A., Stark, H., and Fischer, U. (2008). An assembly chaperone collaborates with the SMN complex to generate spliceosomal SnRNPs. Cell *135*, 497–509.

Ellis, R.J. (2013). Assembly chaperones: a perspective. Philos. Trans. R. Soc. Lond. B Biol. Sci. *368*, 20110398.

Fischer, U., Englbrecht, C., and Chari, A. (2011). Biogenesis of spliceosomal small nuclear ribonucleoproteins. Wiley Interdiscip. Rev. RNA *2*, 718–731.

Gavin, A.C., Aloy, P., Grandi, P., Krause, R., Boesche, M., Marzioch, M., Rau, C., Jensen, L.J., Bastuck, S., Dümpelfeld, B., et al. (2006). Proteome survey reveals modularity of the yeast cell machinery. Nature *440*, 631–636.

Gong, F., and Yanofsky, C. (2002). Instruction of translating ribosome by nascent peptide. Science *297*, 1864–1867.

Grimm, C., Chari, A., Pelz, J.P., Kuper, J., Kisker, C., Diederichs, K., Stark, H., Schindelin, H., and Fischer, U. (2013). Structural basis of assembly chaperone-mediated snRNP formation. Mol. Cell *49*, 692–703.

Harigaya, Y., and Parker, R. (2010). No-go decay: a quality control mechanism for RNA in translation. Wiley Interdiscip. Rev. RNA *1*, 132–141.

Kambach, C., Walke, S., Young, R., Avis, J.M., de la Fortelle, E., Raker, V.A., Lührmann, R., Li, J., and Nagai, K. (1999). Crystal structures of two Sm protein complexes and their implications for the assembly of the spliceosomal snRNPs. Cell *96*, 375–387.

Keenan, R.J., Freymann, D.M., Stroud, R.M., and Walter, P. (2001). The signal recognition particle. Annu. Rev. Biochem. *70*, 755–775.

Mariappan, M., Li, X., Stefanovic, S., Sharma, A., Mateja, A., Keenan, R.J., and Hegde, R.S. (2010). A ribosome-associating factor chaperones tail-anchored membrane proteins. Nature *466*, 1120–1124.

Meister, G., and Fischer, U. (2002). Assisted RNP assembly: SMN and PRMT5 complexes cooperate in the formation of spliceosomal UsnRNPs. EMBO J. *21*, 5853–5863.

Neuenkirchen, N., Englbrecht, C., Ohmer, J., Ziegenhals, T., Chari, A., and Fischer, U. (2015). Reconstitution of the human U snRNP assembly machinery reveals stepwise Sm protein organization. EMBO J. *34*, 1925–1941.

Pechmann, S., Willmund, F., and Frydman, J. (2013). The ribosome as a hub for protein quality control. Mol. Cell *49*, 411–421.

Pillai, R.S., Will, C.L., Lührmann, R., Schümperli, D., and Müller, B. (2001). Purified U7 snRNPs lack the Sm proteins D1 and D2 but contain Lsm10, a new 14 kDa Sm D1-like protein. EMBO J. *20*, 5470–5479.

Pillai, R.S., Grimmler, M., Meister, G., Will, C.L., Lührmann, R., Fischer, U., and Schümperli, D. (2003). Unique Sm core structure of U7 snRNPs: assembly by a specialized SMN complex and the role of a new component, Lsm11, in histone RNA processing. Genes Dev. *17*, 2321–2333.

Rodrigo-Brenni, M.C., and Hegde, R.S. (2012). Design principles of protein biosynthesis-coupled quality control. Dev. Cell *23*, 896–907.

Schuldiner, M., Metz, J., Schmid, V., Denic, V., Rakwalska, M., Schmitt, H.D., Schwappach, B., and Weissman, J.S. (2008). The GET complex mediates insertion of tail-anchored proteins into the ER membrane. Cell *134*, 634–645.

Shieh, Y.W., Minguez, P., Bork, P., Auburger, J.J., Guilbride, D.L., Kramer, G., and Bukau, B. (2015). Operon structure and cotranslational subunit association direct protein assembly in bacteria. Science *350*, 678–680.